ELSEVIER

Journal of Fluids and Structures 26 (2010) 1123–1141

JOURNAL OF FLUIDS AND STRUCTURES

www.elsevier.com/locate/jfs

Investigation of fluid–structure interaction with various types of junction coupling

A. Ahmadi, A. Keramat*

Civil Engineering Department, Shahrood University of Technology, Shahrood, Iran

Received 16 July 2008; accepted 21 August 2010
Available online 20 October 2010

Abstract

In this study of water hammer with fluid–structure interaction (FSI) the main aim was the investigation of junction coupling effects. Junction coupling effects were studied in various types of discrete points, such as pumps, valves and branches. The emphasis was placed on an unrestrained pump and branch in the system, and the associated relations were derived for modelling them. Proposed relations were considered as boundary conditions for the numerical modelling which was implemented using the finite element method for the structural equations and the method of characteristics for the hydraulic equations. The results can be used by engineers in finding where junction coupling is significant.

Keywords: Fluid–structure interaction; Piping systems; Water hammer; Junction coupling

1. Introduction

Transient flow occurs due to a disturbance in the steady flow, such as valve closing or pump shut-down. It can affect the structural piping system due to interaction between the structure and the contained liquid. In the study of fluid–structure interaction (FSI) in piping systems, the most significant mechanism is junction coupling, as compared with the other coupling mechanisms, namely Poisson and friction coupling (Wiggert and Tijsseling, 2001) in the more flexible piping systems (Heinsbroek and Tijsseling, 1994; Heinsbroek, 1997). Junction coupling takes place at unsupported discrete points of the piping systems such as unrestrained valves, branches, closed ends, pumps, etc. The main concept can be numerically implemented by using appropriate boundary conditions which will mutually relate structural and hydraulic values to each other.

FSI in piping systems, considering the effects of column separation, has already been investigated in by Tijsseling (1993). In that study, the method of characteristics (MOC) has been used for numerical modelling of both structural and hydraulic equations. Fan and Tijsseling (1992) have made a study of the simultaneous occurrence of cavitation and FSI. In this research, numerical simulation and experiment concerned a single pipe, while in Tijsseling et al. (1996), a

*Corresponding author.
E-mail addresses: a.ahmadi@shahroodut.ac.ir (A. Ahmadi), alireza.keramat@gmail.com, a.keramat@tue.nl (A. Keramat).

0889-9746/$ - see front matter © 2010 Elsevier Ltd. All rights reserved.
doi:10.1016/j.jfluidstructs.2010.08.002

Nomenclature

A_p (A_f)	cross-sectional area of pipe wall (flow) (m^2)
a	pressure wave speed (m/s)
D	inner diameter of pipe (m)
E	Young's modulus of pipe wall material (Pa)
e	pipe wall thickness (m)
f	Darcy–Weisbach friction coefficient
G	shear modulus of pipe wall material (Pa)
g	gravitational acceleration (m/s^2)
H	piezometric head (m)
I	second moment of cross-sectional inertia (m^4)
I_{pump}	inertia of the pump impeller (kg m^2)
N	rotational speed of pump (rpm)
N_R, T_R, H_R, Q_R	rated quantities of rotational speed, shaft torque, head and discharge
P	fluid pressure (Pa)
Q	discharge (m^3/s)
T	shaft torque of the pump (N m)
V	cross-sectional averaged fluid velocity (m/s)
X, Y, Z	directions of global coordinate system
x	axial direction (x-direction of local coordinate system)
y, z	lateral directions (y-, z-direction of local coordinate system)
α	dimensionless rotational speed
β	dimensionless shaft torque of the pump
γ	weight density of fluid (N/m^3)
Δt	numerical time step, mesh spacing (s)
Δx	element length, mesh spacing (m)
$\eta(w)$	lateral displacement in xz (xy) plane (m)
θ	axial rotation of element (rad)
v	Poisson's ratio
ξ	axial displacement (m)
ρ	fluid mass density (kg/m^3)
τ	temporary opening ratio of valve
υ	dimensionless discharge of pump
$\forall$	cavity volume (m^3)

Matrices and vectors

$\mathbf{C}$	structural damping matrix (kg/s)
$\mathbf{D}$	displacement vector of nodes (m)
$\mathbf{d}^{(e)}$	displacement vector of element (m)
$\mathbf{F}$	load vector in global coordinat system (N)
$\mathbf{f}^{(e)}$	force vector of element (N)
$\mathbf{K}^{(e)}$	stiffness element matrix (N/m)
$\mathbf{M}$	system mass matrix (kg)
$\mathbf{R}^{(e)}$	transformation matrix of element
$\mathbf{S}$	system stiffness matrix (N/m)

Subscripts and superscripts

$\dot{(}$, $\ddot{(}$	first (second) derivative with respect to time
(e)	element properties
f	fluid
glo	global coordinate system
i	spatial discretization index
loc	local coordinate system
n	time discretization index
p	pipe, pump
R	rated quantities (value of its holder is at the point of best efficiency)
val	valve
x, y, z	directions associated with local coordinate system

second pipe was added forming a one-elbow system. The other significant work combining FSI and cavitation by Vardy et al. (1996) concerns a T-piece pipe.

Lavooij and Tijsseling (1991) presented two different procedures for modelling the FSI effects: MOC which is used for both hydraulic and structural governing equations against MOC–FEM where the hydraulic equations are solved by the method of characteristics and the structural equations are solved by the finite element method in combination with a direct time integration scheme. Cases including bends and valves with gradual closure were studied. Furthermore, Heinsbroek (1997) compared two different ways including MOC and FEM for solving the structural equations. The contribution of this work was the comparison of Euler–Bernoulli and Timoshenko beam theories when used in the mentioned ways of solution. This study showed that FSI in pipeline systems can adequately be investigated by application of MOC and FEM for hydraulics and structure of a piping system, respectively. The preceding solution was employed to study the coupling mechanisms in branched piping systems (Keramat, 2006). Jazayeri (2004) gave solutions for hydraulic equations using MOC and structural equations using the control volume method.

In addition to the time-domain analysis such as the present work, many researchers have studied the theoretical and experimental aspects in the frequency domain (Jong, 1994; Zhang et al., 1999). Li et al. (2003) and Tijsseling (2003) have independently solved the main axial FSI equations analytically. In both these studies analytical junction and Poisson coupling modelling has been considered.

An analysis of a two-elbow pipe system done by Moussou et al. (2000) studies perspicuously the effects of junction coupling. Generally, there are many other experimental and numerical researches which have been carried out for

junction coupling considerations with elbows (Tijsseling and Heinsbroek, 1999) but only a few works can be found about investigation of the junction coupling in branched systems.

Here, in the numerical implementation, the junction coupling effect has been taken into account. The main contribution of the present paper is in the appropriately obtained relations proposed for modelling of junction coupling for systems including unrestrained pumps, branches, and valves with gradual closure, which can make its computer implementation convenient and easy. The analysis of junction coupling effects is carried out in three case studies.

2. Basic concepts

2.1. Assumptions

It is assumed that the piping system consists of thin-walled and linearly elastic pipes for which the conventional equations can be used without any further correction (Tijsseling, 2007). Besides, the radial inertia and radial shear deformation of the pipe walls are neglected. The other structural assumptions are that there is no buckling and no large deformations.

In the hydraulic transient analysis, the simplified set of the equations of motion and continuity have been employed for the water hammer numerical implementation (Wylie et al., 1993); the unsteady friction models are not considered here. The discrete vapour cavity model (DVCM) which appears to be simple but adequate can be used to simulate column separation; the underlying hypothesis is that the flow of liquid in the tube is instantaneously and completely separated at the computational sections by its vapour phase when a cavity is formed and there are no cavity bubbles in the regions between the computational sections (Bergant and Simpson, 1999; Bergant et al., 2006).

2.2. Equations

For junction coupling modelling, the hydraulic equations are the formal equations of motion and continuity, but in the case of Poisson coupling modelling, a term – namely the Poisson coupling term – will be added to the continuity equation (Lavooij and Tijsseling, 1989). The governing equations, referred to as extended water hammer, are:

$$\frac{\partial H}{\partial t}+\frac{a^2}{gA_f}\frac{\partial Q}{\partial x}-\frac{2a^2}{g}v\dot{\xi}'=0,\quad \dot{\xi}'=\frac{\partial^2\xi}{\partial x\,\partial t}, \tag{1}$$

$$gA_f\frac{\partial H}{\partial x}+\frac{\partial Q}{\partial t}+f\frac{Q|Q|}{2DA_f}=0. \tag{2}$$

In the above equations Q, H and a are discharge, pressure head and wave velocity and D, A_f, ξ and v are the inner diameter of pipe, cross-sectional flow area, axial pipe displacement and Poisson's ratio, respectively. The above equations include the pressure waves with Poisson coupling, which will interact with the axial, lateral and torsional stress waves which are governed by the following differential equations (Wiggert and Tijsseling, 2001):

$$EA_p\frac{\partial^2\xi}{\partial x^2}-M_p\frac{\partial^2\xi}{\partial t^2}+\frac{A_pvD}{2e}\frac{\partial P}{\partial x}+\frac{\pi Df\rho_f V|V|}{8}+M_pg_x=0, \tag{3}$$

$$GJ_0\frac{\partial^2\theta}{\partial x^2}-J_0\rho_p\frac{\partial^2\theta}{\partial t^2}=0, \tag{4}$$

$$EI\frac{\partial^4 w}{\partial x^4}+M\frac{\partial^2 w}{\partial t^2}+Mg_y=0. \tag{5}$$

The variables in the above equations are: fluid pressure, P, cross-sectional averaged fluid velocity, V, axial displacement, ξ, angle of twist, θ, lateral displacement in the xy plane, w, pipe wall thickness, e, cross-sectional area of pipe, A_p, mass of pipe per unit length, M_p, total mass per unit length, M, Young's modulus of elasticity, E, shear modulus, G, moment of inertia, I, polar second moment of area, J_0, components of gravitational acceleration, g_x, g_y. It must be noted that Eq. (5) concerns bending vibration in the xy plane and that there is a similar equation for

vibration in the xz plane, with the lateral displacement η:

$$EI\frac{\partial^4\eta}{\partial x^4}+M\frac{\partial^2\eta}{\partial t^2}+Mg_z=0. \tag{6}$$

2.3. Junction and Poisson coupling

When a discrete point (junction) has the possibility of moving in the direction of pressure waves, mutual forces between the fluid and pipe system may cause a dynamic interaction which is known as junction coupling. A comprehensive discussion of this subject is given in Sections 3.3 and 4.

As indicated, the Poisson coupling term in the continuity Eq. (1) which is dependent on axial pipe displacement on one hand, and the equation of pipe wall axial vibration (3) which is dependent on contained fluid pressure on the other hand, gives rise to a coupled analysis with converging values for both structural and hydraulic variables. From a physical point of view, the Poisson coupling phenomenon is a radial expansion and contraction of the pipe wall, from which axial stress waves will always be generated. These waves will affect the fluid pressure as the conservation of the mass of liquid (Eq. (1)) shows.

It is obvious that for solely Poisson coupling modelling, only the axial vibration equation (3) must be used in the coupled analysis procedure and there is no need to consider the other structural equations (4)–(6). Hence, if it is intended to model the Poisson coupling only, it is necessary to suppress fluid forces which cause lateral and torsional vibrations, and for this purpose all the discrete points (junctions) of the piping system must be blocked (structurally fixed).

Poisson coupling analysis is implemented herein by making separate subroutines to solve the structural and hydraulic equations, where the coupled procedure for each time iteration is continued until arriving at converged values for both structural and hydraulic variables.

3. Solution procedure

In this section the implemented numerical methods and some significant issues to be used for computer programming will be described.

3.1. Method of characteristics

This method has been used for the numerical implementation of the hydraulic equations (1) and (2). This method eventually results in a finite differences form which can be written along two characteristic lines indicated as C^+ and C^- (Wylie et al., 1993):

$$\begin{cases} C^+ : \ H_i^{n+1}=Cp-Bp\,Q_i^{n+1} \\ C^- : \ H_i^{n+1}=Cm+Bm\,Q_i^{n+1} \end{cases} \Rightarrow H_i^{n+1}=\frac{(Cp/Bp)+(Cm/Bm)}{(1/Bp)+(1/Bm)}, \quad Q_i^{n+1}=\frac{Cp-Cm}{Bp+Bm}, \tag{7}$$

in which Cp, Cm, Bp and Bm are known constants evaluated from the values obtained in the previous time iteration:

$$\begin{aligned} &Cp=H_{i-1}^n+BQ_{i-1}^n+\frac{\Delta t}{g}\left(2a^2v\dot{\xi}_i^{n+1}\right), \quad Bp=B+R\left|Q_{i-1}^n\right|, \quad B=\frac{a}{gA_f}, \\ &Cm=H_{i+1}^n-BQ_{i+1}^n+\frac{\Delta t}{g}\left(2a^2v\dot{\xi}_i^{n+1}\right), \quad Bm=B+R\left|Q_{i+1}^n\right|, \quad R=\frac{f\Delta x}{2gDA_f^2}. \end{aligned} \tag{8}$$

Note that the subscript i and superscript n indicate spatial and time discretization, respectively. It can be seen that the only differences in the relations in (8) as compared with the MOC solution of standard water hammer equations are associated with the Poisson coupling term.

3.2. Finite element method

Using the weighted residual method, in the Galerkin form, the structural equations (3)–(6) can be spatially discretized separately to make a matrix form of the equations. These matrices, which are in the local coordinate system, can be combined to make a matrix-form relation for the structural vibrations of the piping system. This matrix-form equation is written in a global coordinate system using the transformation matrix, which can be obtained in conjunction with the element position. It is clear that all these operations are associated with one pipe element; by assembling all elements of

the piping system, a matrix-form equation in the global coordinate system is derived:

$$\mathbf{M}\ddot{\mathbf{D}}+\mathbf{C}\dot{\mathbf{D}}+\mathbf{S}\mathbf{D}=\mathbf{F}, \tag{9}$$

where **M**, **C** and **S** are the general mass matrix, the general damping matrix and the general stiffness matrix of the total system, respectively; **F** is the load vector and **D** is the unknown vector in the global coordinates of the piping system (the overdot is used for time derivatives). In the present study, in order to analyse Eq. (9) in the time domain, the Newmark-beta time-integration scheme has been implemented. Also to diminish the artificial numerical oscillations, a special form of Rayleigh's damping has been used.

3.3. Coupled analysis procedure

If it is intended to model junction coupling solely, the classical water hammer differential equations will be employed and the only coupling mechanism will be associated with the boundary conditions in such a manner that, on the one hand, the hydraulic boundary conditions must be written considering the structural response and, on the other hand, the structural load vector must be applied considering the fluid pressure. The details of these coupling mechanisms in the boundary conditions and force vector will be discussed in the subsequent sections.

In the case of both Poisson and junction coupling, the extended water hammer equations accompanied by the mentioned boundary conditions must be considered. It is clear that if all discrete points (junctions) are structurally fixed, then no junction coupling will occur. Therefore, with more flexible piping systems, stronger junction coupling effects will occur.

3.4. Post-processing of the solution

Assume that a structural analysis of the piping system has been done and the $\mathbf{D}$, $\dot{\mathbf{D}}$, $\ddot{\mathbf{D}}$ vectors in any time iteration have been obtained. The members of these three vectors are displacements, velocities and accelerations of nodes in the generalized coordinate system, respectively. Using these vectors the unknown support reactions, which play the role of forced boundary conditions, are computed by

$$\mathbf{F}_{\mathrm{r}}=\mathbf{S}\mathbf{D}. \tag{10}$$

For calculating the displacements, velocities and accelerations in the global coordinate system for each element, the inverse operations of those in the assembling procedure should be done, but here the operations are easy. This is understood by the concept of which element is located between which nodes. From doing this operation on the $\mathbf{D}$, $\dot{\mathbf{D}}$, $\ddot{\mathbf{D}}$ vectors, the vectors $\mathbf{d}^{(e)}_{\mathrm{glo}}$, $\dot{\mathbf{d}}^{(e)}_{\mathrm{glo}}$, $\ddot{\mathbf{d}}^{(e)}_{\mathrm{glo}}$ are found for any element. For calculating the displacements, velocities and accelerations in the local coordinate system for any element, the following relations are used:

$$\mathbf{d}^{(e)}_{\mathrm{loc}}=\mathbf{R}^{(e)}\mathbf{d}^{(e)}_{\mathrm{glo}},\quad \dot{\mathbf{d}}^{(e)}_{\mathrm{loc}}=\mathbf{R}^{(e)}\dot{\mathbf{d}}^{(e)}_{\mathrm{glo}},\quad \ddot{\mathbf{d}}^{(e)}_{\mathrm{loc}}=\mathbf{R}^{(e)}\ddot{\mathbf{d}}^{(e)}_{\mathrm{glo}}, \tag{11}$$

in which the matrix $\mathbf{R}^{(e)}$ is the transformation matrix corresponding to any element. What is obtained from Eq. (11) is used to evaluate the Poisson coupling term $\dot{\xi}'$ in Eqs. (1) and (8). Consider in a 3-D piping system the first and seventh members that are related to the axial displacements ($\dot{\xi}_1=\dot{d}_1$, $\dot{\xi}_2=\dot{d}_7$) resulting in $\dot{\xi}'=(\dot{d}_7-\dot{d}_1)/\Delta x$. Finally, the axial and shear forces and torsion and bending moments are evaluated by

$$\mathbf{f}^{(e)}_{\mathrm{loc}}=\mathbf{R}^{(e)}\mathbf{f}^{(e)}_{\mathrm{glo}}=\mathbf{R}^{(e)}\left(\mathbf{K}^{(e)}_{\mathrm{glo}}\mathbf{d}^{(e)}_{\mathrm{glo}}\right), \tag{12}$$

where $\mathbf{K}^{(e)}_{\mathrm{glo}}$ is the stiffness element matrix in the global coordinate system.

4. Numerical modelling of junction coupling

In the modelling of junction coupling, where the steady state flow velocity is changing, the hydraulic and structural boundary conditions must be adapted as follows.

4.1. Hydraulic boundary conditions

The major aspect of this research is to derive appropriate relations for an unrestrained valve, a multi-branch and a pump, to be used as boundary conditions for the hydraulic equations.

4.1.1. Valve placed at the end of a pipe

Assuming an unfixed valve at the end of a pipe which is being closed gradually; then, the following equation can be written using the continuity and energy equation for that discrete point:

$$Q_i^{n+1}=\frac{Q_0\tau}{\sqrt{H_{0,\mathrm{val}}}}\sqrt{H_i^{n+1}-Z_{\mathrm{val}}}+\dot{\xi}_i^{n+1}A_f,\quad H_{0,\mathrm{val}}=\frac{P_0}{\gamma}\big|_{\mathrm{valve}}=H_0\big|_{\mathrm{valve}}-Z_{\mathrm{val}},\tag{13}$$

in which Z_{val} is the elevation of the valve node and the quantities $H_{0,\mathrm{val}}$ and τ are the pressure head and the temporary opening ratio of the valve, respectively. Simultaneous solution of Eqs. (13) and (7, C^+) for obtaining Q_i^{n+1} and H_i^{n+1}will give

$$Q_i^{n+1}=\dot{\xi}_i^{n+1}A_f-\frac{\tau^2Q_0^2Bp}{2H_{0,\mathrm{val}}}+\sqrt{\left(\frac{\tau^2Q_0^2Bp}{2H_{0,\mathrm{val}}}\right)^2+\frac{\tau^2Q_0^2(Cp-Z_{\mathrm{val}})}{2H_{0,\mathrm{val}}}-\frac{\tau^2Q_0^2\dot{\xi}_i^{n+1}A_fBp}{H_{0,\mathrm{val}}}},\tag{14}$$

where $\dot{\xi}_i^{n+1}$ is the axial velocity of the valve node. Taking $\dot{\xi}_i^{n+1}=0$ in Eq. (14) will give the condition of a restrained valve, and if it is imposed that $\tau=0$ the boundary condition will be that of instantaneous valve closure.

4.1.2. Junction

Fig. 1 shows a free-to-move junction J which, due to unsteady flow, has an oscillating velocity along the X direction of the global coordinate system which is denoted by $\Delta\dot{X}_J$. This quantity is computed by the structural subprogram for the piping system. For the boundary conditions representing an unfixed junction, it is necessary to obtain the velocity of the node J in the direction of each pipe element connected to it; see Fig. 1. This is done in a structural subprogram using the transform matrices, $\mathbf{R}^{(e)}$, which are derived for each element connected to the junction. The results are $\dot{\xi}_1$, $\dot{\xi}_2$, $\dot{\xi}_3$, $\dot{\xi}_4$, where the subscripts indicate the element numbers. Using these quantities, the modified fluid continuity equation can be written for the junction. Finally, the simultaneous solution of this continuity equation and the appropriate C^+ and C^- relations (7) in the adjacent pipes will give the following equation:

$$\begin{aligned}&H_J=\frac{(Cp_1/Bp_1)+(Cp_2/Bp_2)+(Cm_3/Bm_3)+(Cm_4/Bm_4)-St}{(1/Bp_1)+(1/Bp_2)+(1/Bm_3)+(1/Bm_4)},\\&St=A_{f_1}\dot{\xi}_1+A_{f_2}\dot{\xi}_2-A_{f_3}\dot{\xi}_3-A_{f_4}\dot{\xi}_4.\end{aligned}\tag{15}$$

This equation can be extended for any desired number of inlet and outlet pipes connected to the junction:

$$H_J=\frac{\sum_{i=1}^{N_{in}}(Cp_i/Bp_i)+\sum_{i=1}^{N_{out}}(Cm_i/Bm_i)-St}{\sum_{i=1}^{N_{in}}(1/Bp_i)+\sum_{i=1}^{N_{out}}(1/Bm_i)},\quad St=\underbrace{\sum_{i=1}^{N_{in}}A_{f_i}\dot{\xi}_i}_{\mathrm{in}}-\underbrace{\sum_{i=1}^{N_{out}}A_{f_i}\dot{\xi}_i}_{\mathrm{out}},\tag{16}$$

in which N_{in} and N_{out} are the number of the inlet and outlet pipes, respectively. Now, like a fixed junction, after calculating H_J^{n+1} in the specific time iteration, the discharges corresponding to each pipe are governed by the C^+ and C^- equations. It is noted that a closed end, a mitre bend and a T-section are special forms of the generic junction.

4.1.3. Pump

Fig. 2 shows a pump with its control valve. Pump control valves operate such that the closure ratio template of the valve (i.e. a butterfly valve disc) is unaffected by the flow or pressure in the line. So, a prescribed time history of valve opening ratio, τ, can be defined. Considering Fig. 2 for handling a pump failure, the equations of C^+ and C^- can be written for the points 1 and 3, respectively. Also, there is a relation for the pump between points 1 and 2 and a relation

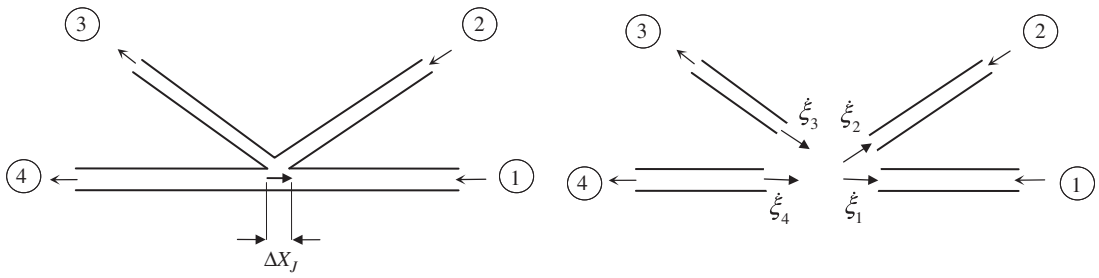

Fig. 1. An unrestrained multi-branch.

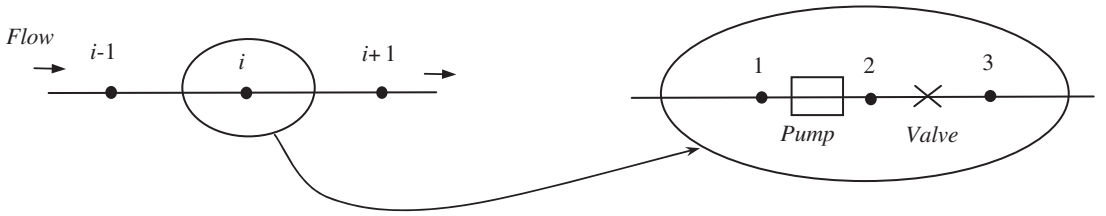

Fig. 2. Pump and its control valve represented as node *i*.

across the valve between points 2 and 3 (Wylie et al., 1993). To obtain the unknowns, including the heads in points 1, 2, 3 and the discharge, all the mentioned relations can be combined to achieve the following nonlinear equations (17) and (19), with the unknowns α and υ to be solved with the Newton–Raphson numerical procedure (see Appendix A):

$$Cp-Cm-Bp\,Q_p-Bm\,Q_v+H_R\left(\alpha^2+\upsilon_p^2\right)(A_0+A_1x)-\frac{\upsilon_v|\upsilon_v|\Delta H_0}{\tau^2}=0,$$
$$\upsilon_v=\frac{Q_v-\dot{\xi}_vA_f}{Q_{\mathrm{R}}},\quad \upsilon_p=\frac{Q_p-\dot{\xi}_pA_f}{Q_R},\quad \alpha=\frac{N}{N_R},\tag{17}$$

in which A_0, A_1 and x are quantities representing the pump characteristics and given by the pump curve and ΔH_0 is the head loss across the valve due to steady flow. N, Q_p and Q_v are rotational speed and discharges of pump and valve, respectively. The subscript R indicates rated quantities. In the above equation, for simplicity, assume that $\upsilon_p=\upsilon_v=\upsilon$. This means that the pump and valve are considered to be connected firmly to each other, with no possibility to change the distance between them. So,

$$\upsilon_p=\upsilon_v=\upsilon,\quad \dot{\xi}_p=\dot{\xi}_v=\dot{\xi}\rightarrow Q_p=Q_v=Q=\upsilon Q_R+\dot{\xi}A_f.\tag{18}$$

With the assumption described in relation (18), another equation which is related to the change of rotational speed of pump is (see Appendix B)

$$(\alpha^2+\upsilon^2)[B_0+B_1x]+\beta_0-C_T(\alpha_0-\alpha)=0,\quad C_T=I_{\mathrm{pump}}\frac{N_R}{T_R}\frac{\pi}{30\Delta t},\quad \beta_0=\frac{T_0}{T_R},\quad x=\pi+\tan^{-1}\frac{\upsilon}{\alpha},\tag{19}$$

where B_0 and B_1 are quantities similar to A_0 and A_1 and T and I_{pump} are the shaft torque and the inertia of the pump impeller. The zero subscripts on the α, β and T refer to values at the earlier time step.

4.2. Structural boundary conditions

In the piping system simulated as a structural frame, fluid pressure multiplied by flow area acts as a concentrated load on a frame junction. It is clear that, where the junction is blocked, displacement is zero and this brings about a direct transmission of the fluid forces to the supports or anchors. Where the junction is free to move, in the simulation, the concentrated loads of the fluid should be entered in the force vector in the position where the related displacements occur. Similarly, forces acting on the pump and its valve during power failure can be evaluated using calculated heads in the nodes 1 and 3, see Fig. 2.

4.3. Column separation

Column separation occurs when the pressure drops to vapour pressure. For simulating this phenomenon numerically, the pressure head was held equal to vapour pressure, and the equations of C^+ and C^- are utilized to calculate discharges at either side of the cavity volume. This volume can be calculated using the following integration scheme for the MOC with staggered grid for the conditions of junction coupling (Tijsseling, 1993):

$$\forall^{n+1}=\forall^{n-1}+2\Delta t\,\{\psi[(Q_2^{n+1}-\dot{\xi}_2^{n+1}A_f)-(Q_1^{n+1}-\dot{\xi}_1^{n+1}A_f)]+(1-\psi)[(Q_2^{n-1}-\dot{\xi}_2^{n-1}A_f)-(Q_1^{n-1}-\dot{\xi}_1^{n-1}A_f)]\},\tag{20}$$

where the subscripts 1 and 2 refer to the discharges upstream and downstream of the cavity volume $\forall$, and ψ is a weighting factor. The described method called DVCM was employed in this research because of its easy implementation and fast computing (Bergant and Simpson, 1999; Bergant et al., 2006). Eq. (20) is a general equation for junctions, bends or other movable pieces in a piping system. For closed ends and check valves, one of the discharges Q_1 or Q_2

should be considered zero. In the case of a pump as a discrete point, various scenarios might take place, e.g. the occurrence of vapour pressure on either side of the pump or on both sides. This case was studied as a separate research on the column separation phenomenon by Keramat et al. (2009).

5. Validation

A computer program using MATLAB software has been developed and all equations presented in this article have been investigated with it. To examine the validity of the described model, the results of two cases presented in Tijsseling (2003), Tijsseling (1993) and Heinsbroek (1997) were compared with those of the present model. The details of this comparison are set out in the next sections.

It is worth noting that the detailed FSI experiments by Fan and Tijsseling (1992), Tijsseling et al. (1996) and Vardy et al. (1996) concern freely suspended pipes with closed ends that are excited by impact loads. Any uncertainties associated with pipe supports, reservoir–pipe connections, valve closure behaviour, dynamic pump characteristics and dissolved and free air are absent in these experiments. However, these complications occur in all practical pipe systems. Separate investigations of the above-mentioned uncertainties in FSI models are therefore needed. In addition, unsteady friction should be investigated in combination with FSI if damping effects are an issue. If such investigations have been carried out successfully, in the near future FSI in practical piping systems can be predicted with an acceptable level of accuracy.

5.1. Benchmark 1

The specifications of a reservoir–pipe–valve system known as Delft Hydraulics Benchmark Problem A are given in Table 1 (Tijsseling, 2003). It was used to test the numerical method and the present software. This model has been solved to investigate junction coupling. For this aim, the valve was considered to be free to move. In Fig. 3 the results obtained for pressure head at valve and midpoint were validated against the exact solution of Tijsseling (2003) who provided the authors with his results. The reason of the dissimilarities which are merely in the discontinuities is due to the fact that basically the finite element method cannot capture sufficiently well the instantaneous variations.

Table 1
The properties of the pipeline according to the case study in Tijsseling (2003).

Length	Diameter	Thickness	Pipe density	Young's modulus	Poisson ratio	Wave velocity	Steady state velocity	Reservoir head
20 m	797 mm	8 mm	7900 kg/m^3	2.1×10^{11} Pa	0.0	1024.7 m/s	1 m/s	0 m

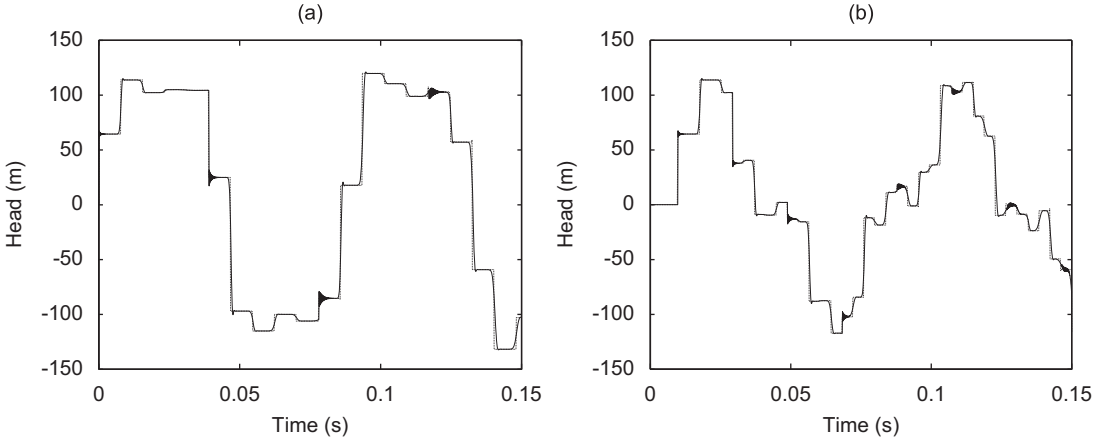

Fig. 3. Pressure head comparison of present and exact (Tijsseling, 2003) solution in continuous and broken lines, respectively.

5.2. Benchmark 2

In Fig. 4, the system to be analysed is sketched (Tijsseling, 1993; Heinsbroek, 1997) and the numbers of nodes are shown. In this model called Delft Hydraulics Benchmark Problem D, the pipes and elbow are allowed to move freely in the horizontal (Y–Z) plane and the valve is rigidly fixed to the ground. The long and short pipes are 310 and 20 m long, respectively. The valve closure time is 0.5 s. The other specifications are listed in Table 2. Accordingly, the computed pressure wave speed is 1192 m/s.

In Figs. 5 and 6 the computed time histories of the analyses without coupling, with junction coupling and with Poisson and junction coupling, for two dynamic displacement components at the elbow are compared with those of

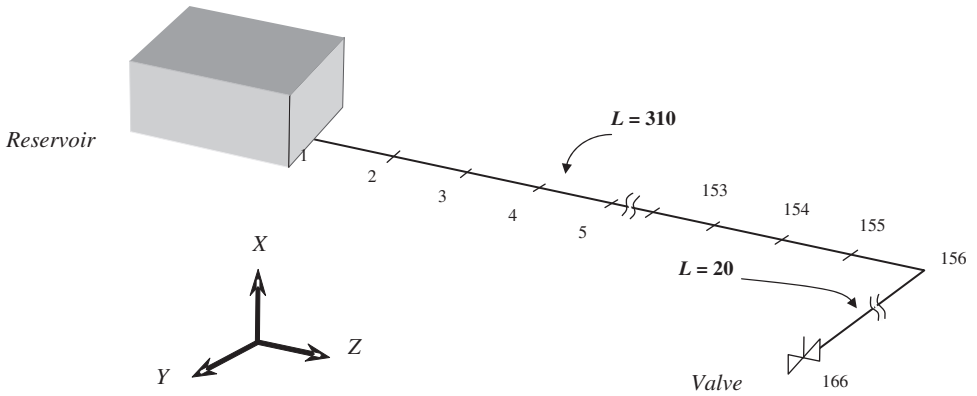

Fig. 4. Pipeline system in benchmark 2.

Table 2
The properties of the pipeline according to the case study in Heinsbroek (1997).

Diameter	Thickness	Pipe density	Fluid density	Young's modulus	Bulk modulus	Poisson ratio	Steady state discharge	Friction coefficient	Reservoir pressure head
206.4 mm	6.35 mm	7900 kg/m^3	880 kg/m^3	2.1×10^{11} Pa	1.55×10^9 Pa	0.3	0.1338 m^3/s	0.02	26.23 m

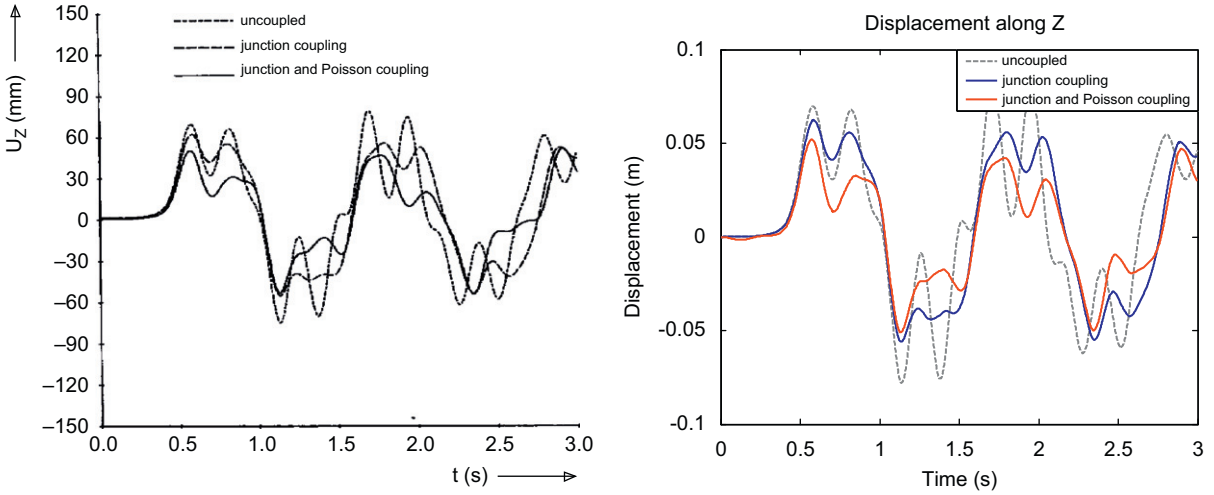

Fig. 5. Comparison of Z-displacement at the elbow, results of FLUSTRIN to the left (provided by Dr. Tijsseling) and results of present study to the right.

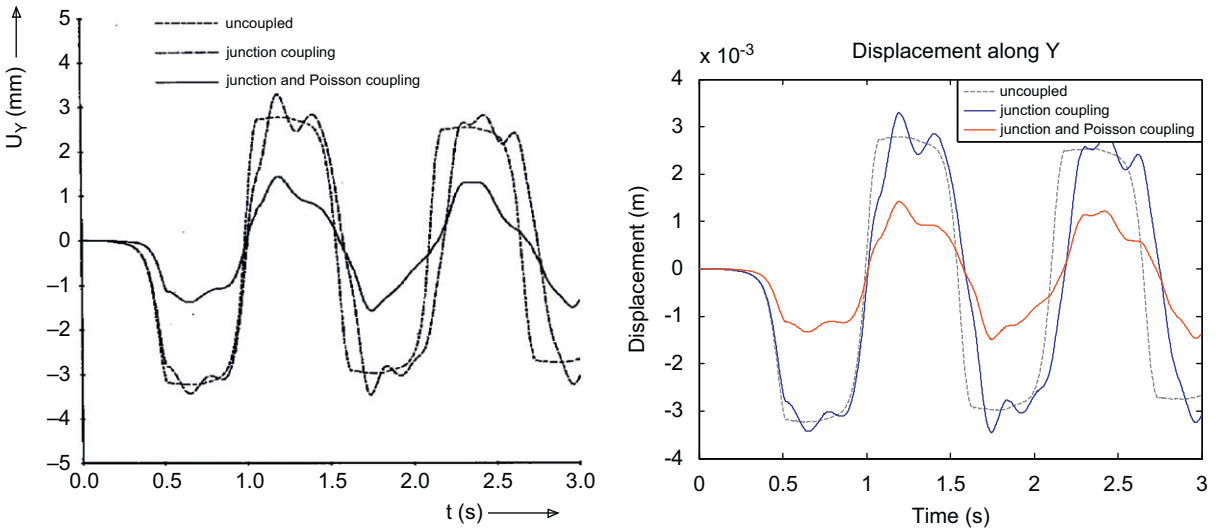

Fig. 6. Comparison of *Y*-displacement at the elbow, results of FLUSTRIN to the left (provided by Dr. Tijsseling) and results of present study to the right.

FLUSTRIN, a verified code provided by Delft Hydraulics Laboratory. As seen, both results show very good agreement with each other.

6. Case studies

Three model problems were considered to be solved for the investigation of junction coupling at valve, branch and pump. The first model was presented to illustrate FSI for gradual valve closure. The second model was introduced to investigate the junction coupling effects of branches, and the third one was given to scrutinize the junction coupling in a system including a failing pump.

6.1. Case study 1

Junction coupling effects of benchmark 1 with now a steady pressure head of 50 m, was scrutinized for the case of gradual valve closure. The valve was closed in 0.03 s and in 0.05 s, and for simplicity, τ was considered as a linear function of time in Eqs. (13) and (14). Fig. 7(a–d) compares the results for gradual closure of the valve with those of instant closure.

Fig. 7(a) shows that in the case of rapid closure and not considering the FSI, the maximum pressure rise is the same for both instant and gradual closure. In fact, when the closure time is less than $2l/a$ (where l is the pipe length and a is the pressure wave speed), the time of valve closure, t_c, has no effect on the maximum pressure rise. This fact is also true for the junction coupling case as shown in Fig. 7(b), but in the junction coupling case, the $2l/a$ criterion can be different depending upon the variation of fundamental frequency, which in turn depends on the rigidity of the piping system. The support rigidity of piping systems has been investigated by Heinsbroek and Tijsseling (1994), and it is also further investigated in the second case study of this research. In the case of slow valve closure for both cases: with and without FSI, the maximum pressure rise is smaller than in the corresponding cases for instant valve closure; see Fig. 7(c) and (d). Therefore, one difference between the calculations with and without FSI for gradual valve closure is the criterion of $2l/a$ which, as argued, may differ due to junction coupling.

Fig. 8 shows the variation of pressure head in the middle of the pipeline for the condition of junction coupling in the case of rapid and slow valve closures. It confirms the fact that the fundamental frequency changes because of junction coupling, which changes the $2l/a$ criterion of distinguishing between rapid and slow valve closure slightly. This also could be understood by comparing Fig. 7(c) and (d).

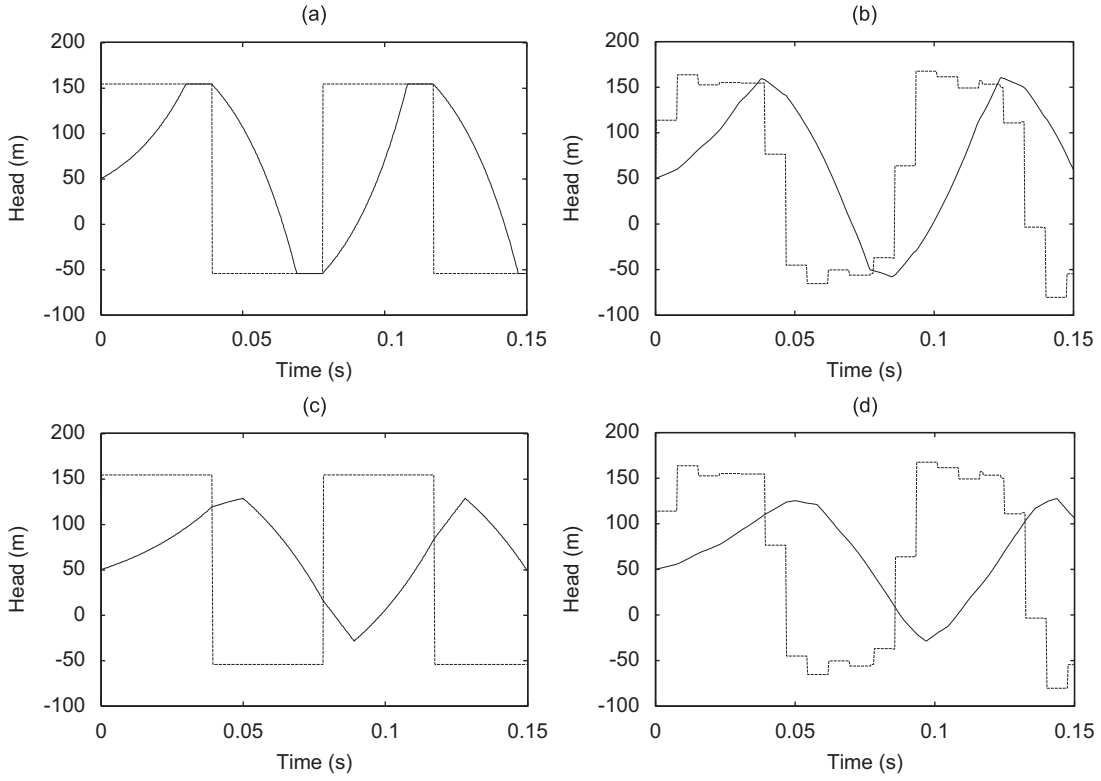

Fig. 7. Comparison of heads at valve due to rapid and slow valve closure under the conditions of no-FSI and of junction coupling; broken lines are for instantaneous valve closure.

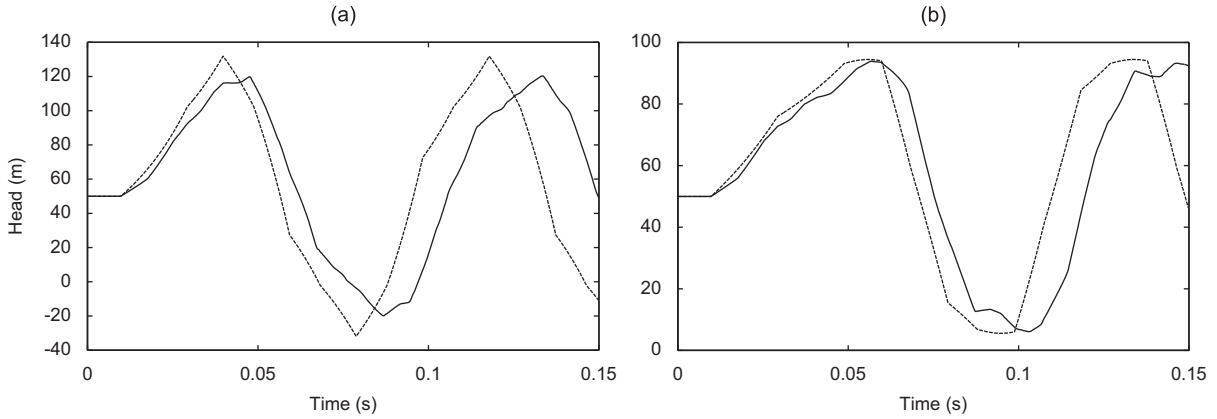

Fig. 8. Head at the middle of the pipeline for gradual valve closure with junction coupling: $t_c = 0.03$ s to the left and $t_c = 0.05$ s to the right. Broken lines are the results of classical water hammer.

6.2. Case study 2

In this model problem the first aim was to illustrate the effects of junction coupling due to water hammer occurring in a branched system excited by valve closure. The system consists of a reservoir establishing the flow in a main pipeline which via a branch is linked to two other pipelines, one ending with a consumer and the other ending with a valve. The specifications of the piping system are given in Table 3 and the number of elements and the length of each one in the

Table 3
The properties of the piping system depicted in Fig. 9.

Discharge of main pipe	Discharge of branches	Diameter of all pipes	Thickness of all pipes	Pipe density	Young's modulus	Wave velocity	Reservoir pressure head
0.020 m^3/s	0.010 m^3/s	200 mm	8 mm	8000 kg/m^3	2.1×10^{11} Pa	1271 m/s	50 m

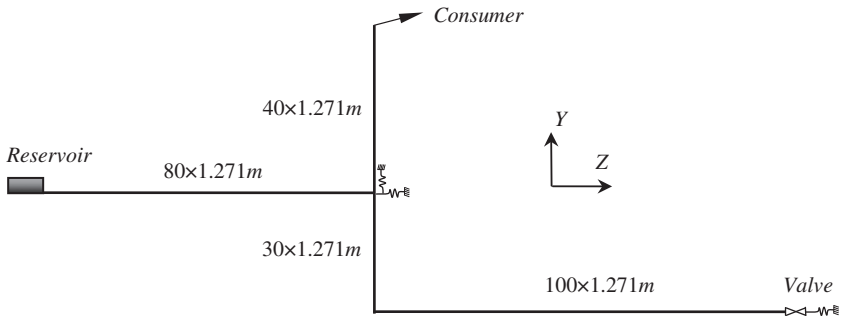

Fig. 9. The geometrical properties of the piping system in case study 2. For each pipe, the number of elements in the simulation and the length of each one are indicated.

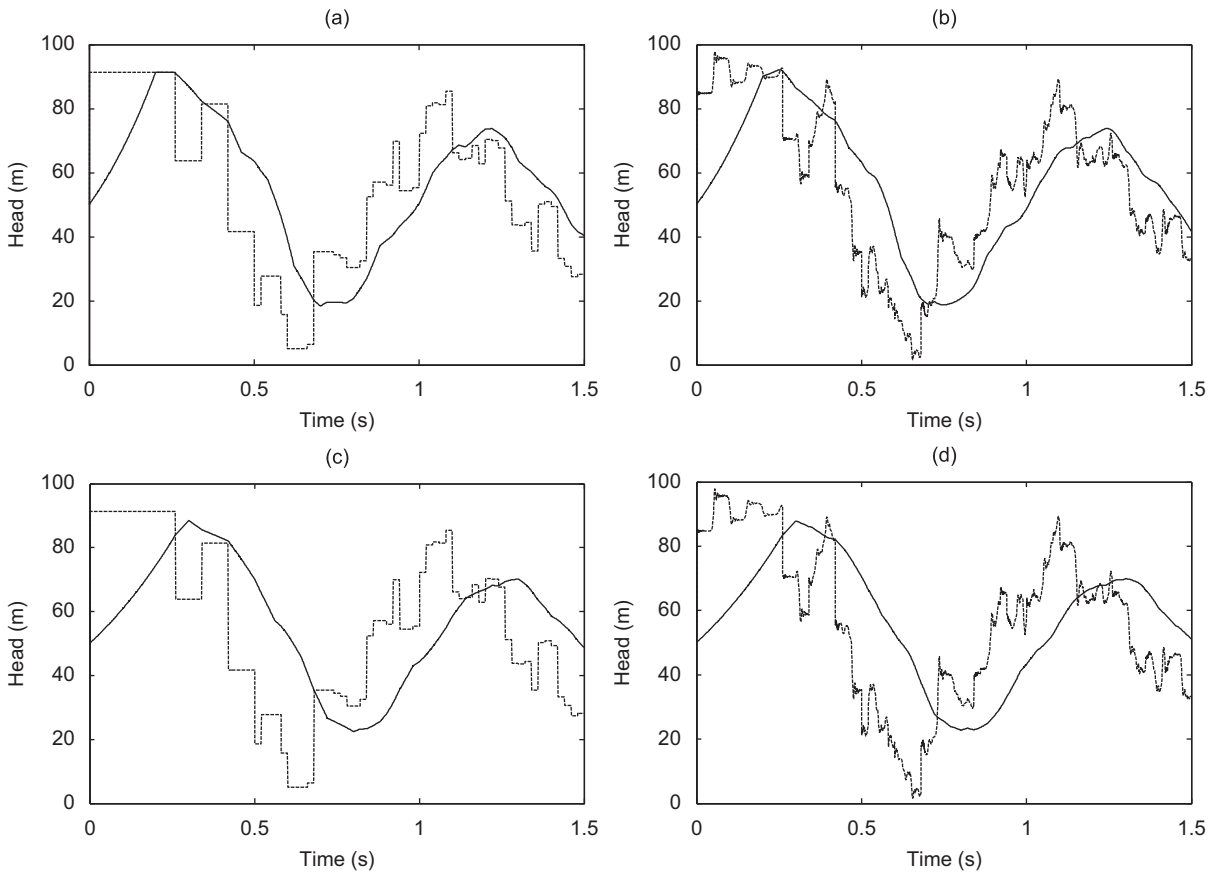

Fig. 10. Comparison of heads for two different durations of valve closure under the conditions of no-FSI and of junction coupling; broken lines are for instantaneous closure.

numerical analysis are depicted in Fig. 9. For modelling only junction coupling, the Poisson ratio of all pipes is set equal to zero, and under this circumstance, branch and valve are allowed to move and other connections including the reservoir, consumer and bend are assumed to be restrained.

In an attempt to study the effects of valve closure, the piping system was solved for two different closure times and the results are shown in Fig. 10; broken lines are for instantaneous valve closure. From the results it can be seen that in a branched system, the time for the wave to travel to and fro, between valve and the nearest (reflection) point releasing the high pressure, is the time of establishment of high pressure produced by valve closure, which in this case is $2 \times (130 \times 1.271/1271) = 0.26$ s. This in fact provides a criterion for valve closure for this model. It can be concluded that, if the valve closure time takes less than this criterion, the system will experience the high pressure (full Joukowsky) even for a very short time (Fig. 10(a) and (b)), otherwise the lower pressure of the reflected wave will reach the valve, and the high pressure will never occur (Fig. 10(c) and (d)). The other comparison between the results with and without junction coupling provided in Fig. 10 leads to the conclusion that valve gradual closure would cause a kind of damping effect on junction coupling so that, for closures with more delay, the results for junction coupling included and not-included are approximately alike. Taking notice of the existence of a consumer in this case study, pressure reductions with time, seen in all of the results, could be inferred.

The second aim was to investigate the influence of the rigidity of piping system on junction coupling. Rigidity relates to structural parameters of the system, such as pipe wall thickness, modulus of elasticity and the stiffness of supports. To illustrate the effects of rigidity, two different values for the support stiffness of branch and valve and modulus of elasticity were taken into account and the results are shown in Fig. 11(a) and (b). Support rigidities were modelled by two different springs with stiffnesses $k_Y = k_Z = k1 = 0$ N/m and $k_Y = k_Z = k2 = 10^7$ N/m placed at the branch and valve (Fig. 9).

From the results, it can clearly be understood that the number of rises and drops due to junction coupling varies with pipe modulus of elasticity, as in the initial time interval of 0.26 s, the number of rises and drops are around five for $E = 2.1 \times 10^{11}$ Pa and four for $E = 1.1 \times 10^{11}$ Pa. This is as a consequence of a higher stress wave speed in a more rigid material. Turning to the influence of support stiffness on junction coupling, the story is different. It results in the sloping pressure ascents or descents instead of the drastic ones revealed for systems including freely moving discrete points.

To describe junction coupling for this problem, it should be noted that, after the instantaneous valve closure, water hammer results in a pressure rise that pushes the valve forward, so the increase in pressure will initially be smaller than that of classical water hammer. The structural wave originating from the pushed valve will travel to the bend and back to the valve; this movement lasts around 0.05 s for the piping system of Fig. 11(a) and around 0.07 s for the system of Fig. 11(b). The returned wave pulls the valve back and decreases the storage capacity for fluid at the valve and establishes higher pressure than classical water hammer.

Basically, changes in fluid velocity cause the water hammer event which in turn can result in raising the pressure and deforming the shape of the structure of the pipe system. The amount of initial pressure rise or distortion depends on the

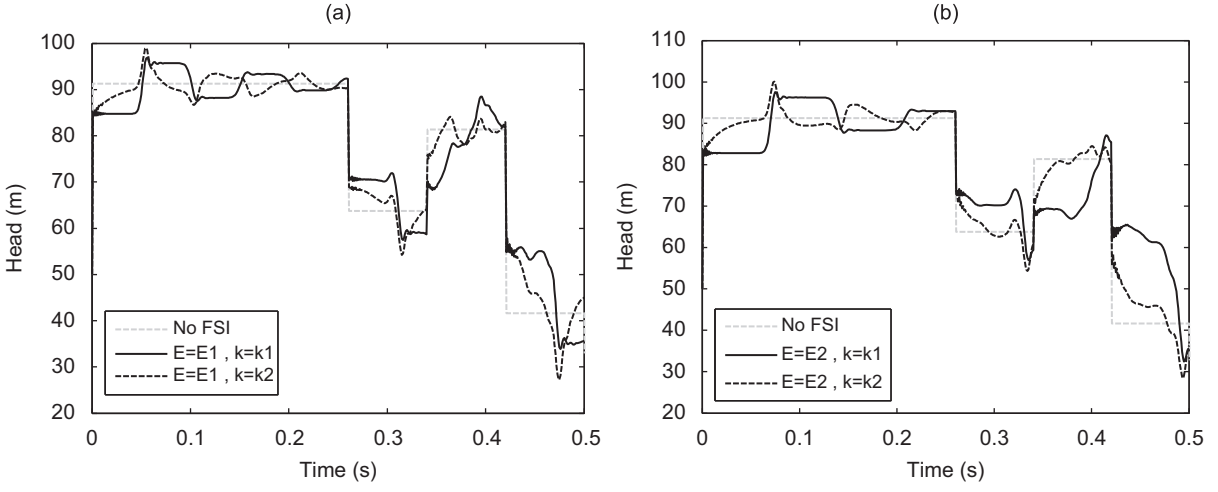

Fig. 11. Comparison of heads for systems with different structural rigidities, $E1 = 2.1 \times 10^{11}$ Pa, $E2 = 1.1 \times 10^{11}$ Pa and $k1 = 0$, $k2 = 10^7$ N/m (for the branch and valve).

rigidity of the structure. In soft systems, the water hammer event can bring about larger deformations and smaller initial pressure rises as compared with rigid systems.

6.3. Case study 3

In an attempt to investigate the effects of junction coupling due to water hammer caused by a pump failure, a pipeline as shown in Fig. 12 was considered. The specifications of this model are given in Table 4. As discussed in Section 4.1.3, the pump and its control valve, referred to as the pump, cannot move relative to each other. A fifth-order polynomial pattern was considered for valve closure within 7 s.

When the pump works at steady state, it develops a total dynamic head increase of 73.2 m from suction flange to discharge flange and establishes the flow of 0.221 m^3/s. Pump failure causes water hammer events at downstream and upstream sides of pump which are examined in Figs. 13 and 14, respectively. As shown, it generates rarefaction waves to be transmitted downstream and pressure waves to be transmitted upstream. These two waves interact, depending on the length of inlet and outlet pipes, before the full closure of the valve. The first interaction can be recognized by a discontinuity in slope as seen in Fig. 13(a) at about $t = 1$ s. As time progresses, due to the reactive torque of the liquid on the impeller, its rotational speed will decline, which in turn results in the same pressures at either side of pump (compare Figs. 13(a) and 14(a)) and at the same time, discharge tends to reduce. Ideally, the control valve should be closed when the fluid velocity is zero or back flow is going to be initiated, because under these circumstances no water hammer is generated due to valve closure and the only existing water hammer is due to the reflected waves of pump failure. However, in practical cases it is recommended that the control valve should be closed 3–5 times slower than the critical period $2l/a$ to minimize the surge, and it also should not be closed so slowly that back flow occurs. In this example, the control valve fully closes a bit before fluid velocity becomes zero, thus it causes instantaneous head drop shown in Fig. 13(a) and rise in Fig. 14(a) at $t = 7$ s. If the valve closes just when the fluid velocity is zero, all the instantaneous jumps are eliminated from the solutions.

Taking notice to solutions with only junction coupling of the pump presented in Figs. 13(b) and 14(b) leads to the fact that it cannot be significant before full closure of the valve, because it is analogous to junction coupling of a valve with gradual closure (case study 1); which, as shown, it was not very different from classical water hammer results. But following the valve full closure, a significant water hammer occurs at either side of the valve, which causes the pressure drop at the downstream side of the valve and the pressure rise at the upstream side (provided that back flow does not occur). These combined pressure drops and rises exert extreme hydraulic forces on the pump system because of their opposite values and leads to pump movements and pressure fluctuations as seen in Figs. 13(b) and 14(b). A slight change in the main frequency due to junction coupling reported in the literature (Heinsbroek and Tijsseling, 1994) can also be confirmed in this example. In general, the intensity of junction coupling arising from pump failure increases by the occurrence of higher pressure change at the pump (difference between pressure rise and drop at either side of the pump). The results of not considering junction coupling and column separation in Figs. 13(a) and 14(a) are drawn as a broken curve in the other related graphs.

In terms of column separation, Figs. 13(c) and 14(c), it is worthwhile to mention that, having transmitted the low pressure wave, cavity bubbles are generated by the pressure reaching vapour pressure at some points along the suction or discharge lines. In this example, according to its specific profile, the cavity will never take place at the points near the pump before the valve full closes. Therefore, small changes in maximum and minimum pressures at the pump are due to cavity volumes along the pipelines, and not at the pump.

Figs. 13(d) and 14(d) show the results for considering both junction coupling and column separation. To make a review on these, fluctuations and changes in maximum and minimum pressures due to column separation and small pressure spikes and changes in the frequency due to junction coupling are partially combined to produce them.

Fig. 15 demonstrates the displacements and support reactions at the pump for two different support rigidities. Only junction coupling and no column separation were involved here. The small oscillations in these graphs before the valve fully closes which

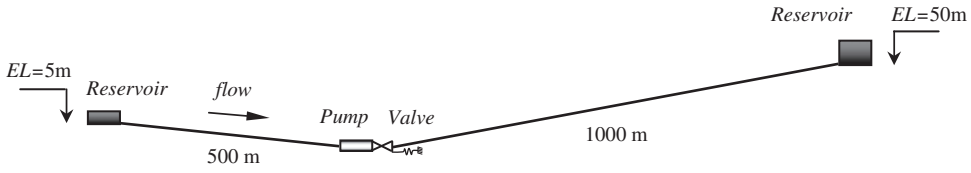

Fig. 12. The geometry of the pipeline in case study 3.

Table 4
The properties of the piping system shown in Fig. 12.

N_R	T_R	H_R	Q_R	I_{pump}	Pump elevation	Pump support stiffness	Valve loss coef.	Downstream res. head	Upstream res. head
1760 rpm	991.6 N m	94.55 m	0.1787 m^3/s	7.9 kg m^2	0 m	0 N/m	0.3	60 m	10 m

Downstream reservoir elevation	Upstream reservoir elevation	Wave velocity	Darcy–Weisbach friction coefficient	Young's modulus	Pipe density	Thickness	Diameter
50 m	5 m	1098 m/s	0.01	2.1×10^{11} Pa	8000 kg/m^3	10 mm	305 mm

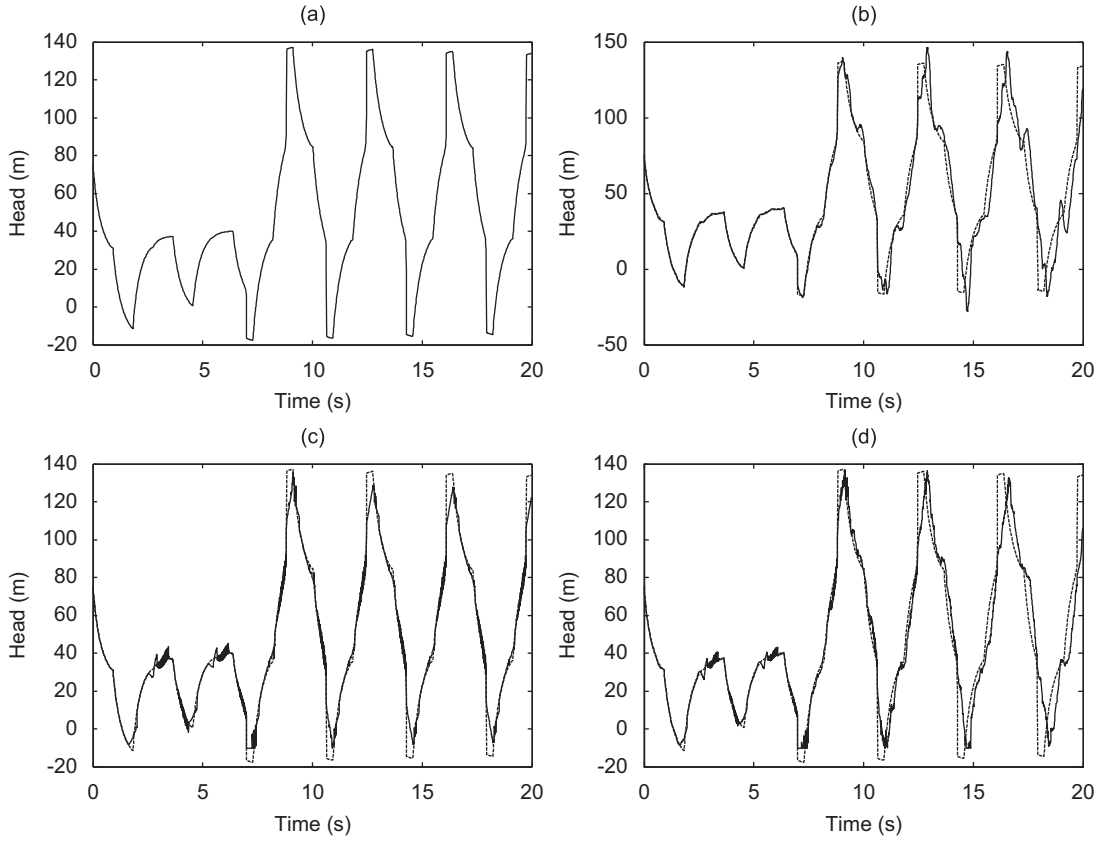

Fig. 13. Head at the downstream side of pump: (a) without junction coupling (JC) and without column separation (CS); (b) with JC and without CS; (c) without JC and with CS; (d) with JC and with CS.

become larger after full closure, are associated with junction coupling. They tend to be diminished with a larger value for support stiffness, as shown. Considering Fig. 15(b) and comparing the rigidities used for the pump support shows that the water hammer effects due to valve closure can be reduced using an adjustable support, operating similar to a spring, for the pump and its control valve.

7. Conclusions

The major goal of this paper was to perform an extensive research on the concept of junction coupling and to scrutinize it for conditions of gradual valve closure in branched systems with different rigidities and systems including a pump. A MOC–FEM procedure was used as numerical solution since hydraulic and structural equations were solved separately in each time step; this in fact has the advantage of easily implementing all available developments on water hammer such as cavitation, unsteady friction, blockage, leakage and viscoelastic behaviour of pipe wall material, in conjunction with junction coupling. Poisson coupling was not considered herein. The results of this research can be used to assist engineers in finding an overall perspective about junction coupling effects. The following conclusions may be drawn.

1. Junction coupling can cause the establishment of pressures a bit higher than the pressures predicted by classical water hammer, so coupled analyses should be made for more sensitive systems.
2. In most cases of branched piping systems, the time it takes for the pressure wave to travel to the branch and back to the valve can be considered as a criterion for rapid or slow closure instead of the $2l/a$ time scale for reservoir–pipe–valve systems. Also due to junction coupling, this criterion may be altered because of changes in the fundamental frequency of water hammer.

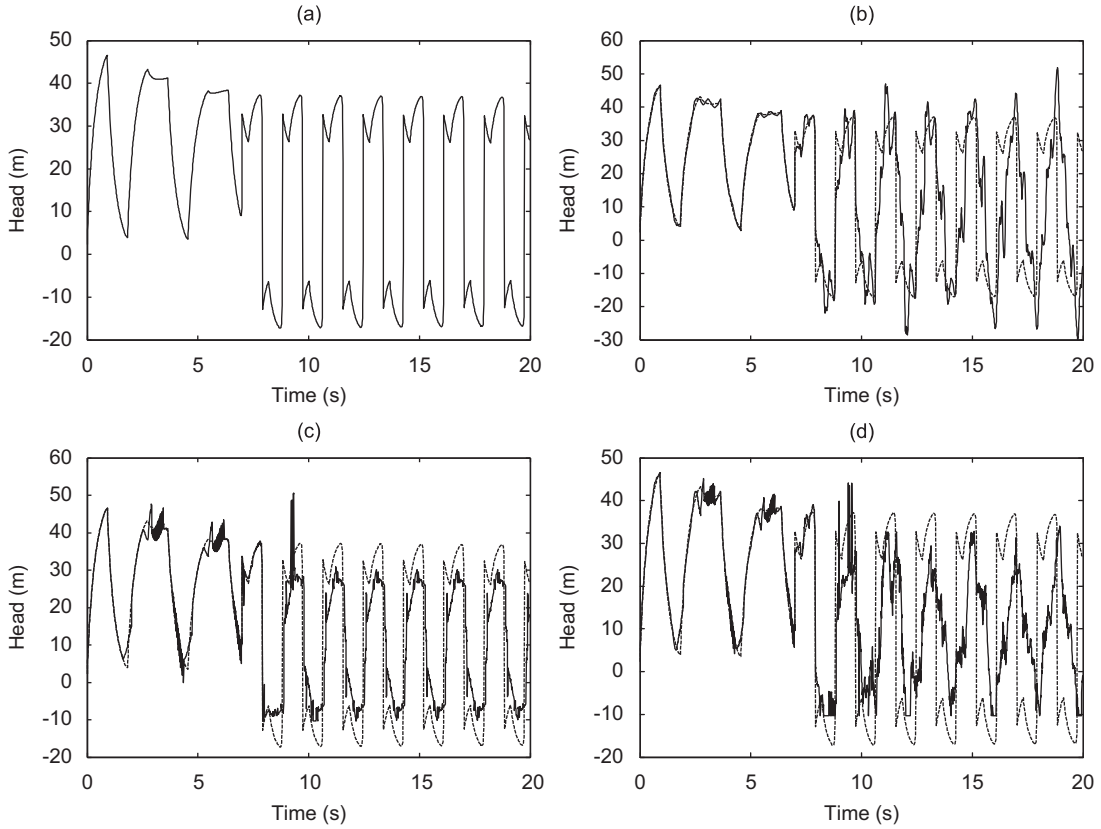

Fig. 14. Head at the upstream side of pump: (a) without junction coupling (JC) and without column separation (CS); (b) with JC and without CS; (c) without JC and with CS; (d) with JC and with CS.

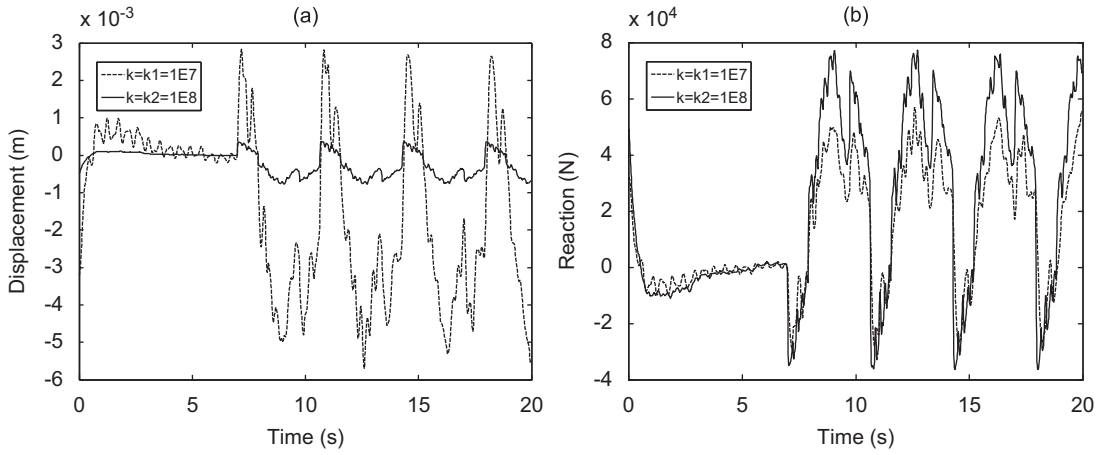

Fig. 15. (a) Comparison of displacements for support rigidities $k1 = 10^8$ N/m and $k2 = 10^7$ N/m in continuous and broken graphs, respectively; (b) comparison of reaction forces for $k1 = 10^8$ N/m and $k2 = 10^7$ N/m in continuous and broken, respectively.

3. Junction coupling is highly dependent on the rigidity of the pipe system. In quite rigid systems, junction coupling does not happen, whereas in very soft systems water hammer results in significant deformation of the piping system and in most such cases, the pressure rises will be small.

4. Interaction of the fluid and structure at the pump location arising from pump failure is mainly contributed to by the operation of the control valve, because of the opposite pressures produced at either side of it. It can be limited by a suitable selection of its closure time.

Acknowledgements

The thoughtful comments and revisions made by Dr. Tijsseling are very much appreciated. Thanks are also due to Professor H.M.V. Samani and Mr. A. Majd for their helps and comments.

Appendix A. Derivation of Eq. (17)

To do a transient analysis for a system including a pump, it is necessary to have the pump characteristics for a particular rotational speed. Then, homologous relations are used to find the characteristic curves at different speeds. As homologous equations are difficult to handle directly, first, four nondimensional quantities are defined as

$$h=\frac{H}{H_R},\quad \beta=\frac{T}{T_R},\quad \upsilon_p=\frac{Q_p-\dot{\xi}_p A_f}{Q_R},\quad \alpha=\frac{N}{N_R}, \tag{A1}$$

in which $\dot{\xi}_p$ is the axial velocity of pump vibration along the pipeline and $\upsilon_p=\upsilon$ according to relation (18); then, the pump characteristics are plotted in terms of $\tan^{-1}(\upsilon/\alpha)$ versus $h/(\upsilon^2+\alpha^2)$ or $\beta/(\upsilon^2+\alpha^2)$, giving the head or torque. Subsequently, using a linear extrapolation for previous calculations of α and υ, the following relation is written to represent the characteristic pump head according to its germane curve:

$$\frac{h}{\alpha^2+\upsilon^2}=A_0+A_1 x,\quad x=\pi+\tan^{-1}\left(\frac{\upsilon}{\alpha}\right), \tag{A2}$$

where A_0 and A_1 are constants which for the first try of the current time step are obtained by the assumed straight line defined through the two adjoining data points of υ and α of the previous time step (Wylie et al., 1993).

For handling the pump failure, considering Fig. 2, except for equations C^+ and C^-, there is relation (A3) for the pump between points 1 and 2, as well as (A4) across the valve between points 2 and 3:

$$H_1+hH_R=H_2, \tag{A3}$$

$$H_2-\frac{(Q_v-\dot{\xi}_v A_f)\left|Q_v-\dot{\xi}_v A_f\right|\Delta H_0}{\tau^2 Q_0^2}=H_3 \tag{A4}$$

with the head loss across the valve equal to ΔH_0 when the flow is Q_0 and $\tau=1$. Here again $\dot{\xi}_v$ is the velocity of valve vibration along the pipeline. With replacing for h from (A2) in (A3) and calculation using relations C^+ and C^- for H_1 and H_3 in Eqs. (A3) and (A4), respectively, and removing H_2 between them, Eq. (17) is obtained.

Appendix B. Derivation of Eq. (19)

There is a differential equation for the pump joining the applied torque to the angular velocity:

$$T=-I_{\text{pump}}\frac{d\omega}{dt},\quad \omega=\frac{2\pi N}{60}. \tag{B1}$$

The above relation has to be integrated numerically because the applied torque, T, is affected by the flow discharge and is a function of time. If integrated using the trapezoidal rule form time t_0 to t_1, the result is

$$\frac{1}{2}[T(t_0)+T(t_1)](t_1-t_0)=-I_{\text{pump}}\frac{2\pi}{60}[N(t_1)-N(t_0)]. \tag{B2}$$

When written using nondimensional quantities, and working with a staggered grid and using the zero-index to represent the values at the previous time step, the following equation:

$$\beta+\beta_0-\frac{\pi N_R I_{\text{pump}}}{30 T_R \Delta t}(\alpha_0-\alpha)=0 \tag{B3}$$

is obtained. And again, like Eq. (A2), there is a relation to represent the torque using a linear extrapolation:

$$\frac{\beta}{\alpha^2+\upsilon^2} = B_0 + B_1 x, \quad x = \pi + \tan^{-1}\left(\frac{\upsilon}{\alpha}\right). \tag{B4}$$

Substitution for β from (B4) into (B3) results in Eq. (19) (Wylie et al., 1993).

References

Bergant, A., Simpson, A.R., Tijsseling, A.S., 2006. Water hammer with column separation: a historical review. Journal of Fluids and Structures 22, 135–171.

Bergant, A., Simpson, A.R., 1999. Pipeline column separation flow regimes. ASCE Journal of Hydraulic Engineering 125, 835–848.

Fan, D., Tijsseling, A.S., 1992. Fluid–structure interaction with cavitation in transient pipe flows. ASME Journal of Fluids Engineering 114, 268–274.

Heinsbroek, A.G.T.J., 1997. Fluid–structure interaction in non-rigid pipeline systems. Nuclear Engineering and Design 172, 123–135.

Heinsbroek, A.G.T.J., Tijsseling, A.S., 1994. The influence of support rigidity on waterhammer pressures and pipe stresses. Proceedings of the Second International Conference on Water Pipeline Systems, BHR Group, Edinburgh, UK, 17–30.

Jazayeri, M.M., 2004 Simultaneous solution of transient flow and structural vibrations of a piping system. M.Sc. Thesis, Civil Engineering Department, Shahid Chamran University of Ahvaz, Iran.

Jong, C.A.F. de, 1994 Analysis of pulsations and vibrations in fluid-filled pipe systems. Ph.D. Thesis, Eindhoven University of Technology, Department of Mechanical Engineering, The Netherlands.

Keramat, A., 2006 Dynamic analysis of fluid-filled piping systems. M.Sc. Thesis, Civil Engineering Department, Shahid Chamran University of Ahvaz, Iran.

Keramat, A., Ahmadi, A., Majd, A., 2009 Transient cavitating pipe flow due to a pump failure. In: Proceedings of the Third IAHR International Meeting of the Work Group on Cavitation and Dynamic Problems in Hydraulic Machinery and Systems, Brno, Czech Republic, October 2009.

Lavooij, C.S.W., Tijsseling, A.S., 1989 Fluid–structure interaction in compliant piping systems. In: Proceedings of the Sixth International Conference on Pressure Surges, BHRA, Cambridge, UK, pp. 85–100.

Lavooij, C.S.W., Tijsseling, A.S., 1991. Fluid–structure interaction in liquid-filled piping systems. Journal of Fluids and Structures 5, 573–595.

Li, Q.S., Yang, K., Zhang, L., 2003. Analytical solution for fluid–structure interaction in liquid-filled pipes subjected to impact-induced water hammer. ASCE Journal of Engineering Mechanics 129, 1408–1417.

Moussou, P., Vaugrante, P., Guivarch, M., Seligmann, D., 2000. Coupling effects in a two elbows piping system. In: Proceedings of the Seventh International Conference on Flow-Induced Vibration, Lucerne, Switzerland, pp. 579–586.

Tijsseling, A.S., 1993 Fluid–structure interaction in case of water hammer with cavitation. Ph.D. Thesis, Delft University of Technology, The Netherlands.

Tijsseling, A.S., 2003. Exact solution of linear hyperbolic four-equation system in axial liquid-pipe vibration. Journal of Fluids and Structures 18, 179–196.

Tijsseling, A.S., 2007. Water hammer with fluid–structure interaction in thick-walled pipes. Journal of Computers and Structures 85, 844–851.

Tijsseling, A.S., Heinsbroek, A.G.T.J., 1999 The influence of bend motion on water hammer pressures and pipe stresses. In: Proceedings of the Third ASME/JSME Joint Fluids Engineering Conference, San Francisco, USA.

Tijsseling, A.S., Vardy, A.E., Fan, D., 1996. Fluid–structure interaction and cavitation in a single-elbow pipe system. Journal of Fluids and Structures 10, 395–420.

Vardy, A.E., Fan, D., Tijsseling, A.S., 1996. Fluid–structure interaction in a T-piece pipe. Journal of Fluids and Structures 10, 763–786.

Wiggert, D.C., Tijsseling, A.S., 2001. Fluid transients and fluid–structure interaction in flexible liquid-filled piping. ASME Applied Mechanics Reviews 54, 455–481.

Wylie, E.B., Streeter, V.L., Suo, L., 1993. In: Fluid Transients in Systems. Prentice Hall, Englewood Cliffs, NJ.

Zhang, L., Tijsseling, A.S., Vardy, A.E., 1999. FSI analysis of liquid-filled pipes. Journal of Sound and Vibration 24, 69–99.